Chapter 1

Lattice methods in fluid dynamics

In the lattice methods, the fluid flow is regarded at the mesoscopic level as a dynamic of the system of special particles with simple properties.

The lattice gas automata (LGA) was for the first time proposed in 1976 [15]. There, the square lattice was used. This model has, however, some drawbacks, the main of them is the unphysical form of the pressure tensor caused by insufficient lattice symmetry. The rapid development of the LGA method began from the work [16] (1986), where the triangular lattice was introduced with the sufficient symmetry (at present, hundreds of papers were published).

The method of lattice Boltzmann Equation (LBE) has grown historically as a development of the lattice gases [17, 18]. This method progresses rapidly during last 15 years. It is very promising for simulation of subsonic liquid flows, especially flows in complex geometry and dynamics of multiphase fluids.

1.1 Lattice gas method

In the LGA method, fluid is modeled microscopically as a collection of particles moving on a regular lattice along the links. There is a small number of possible particle velocity vectors $\mathbf{c}_k$ $(k = 1, \ldots, b)$. The velocity of each particle points to one of the neighbor nodes, and it is chosen so as $\mathbf{c}_k \Delta t = \mathbf{e}_k$ where $\mathbf{e}_k$ are vectors linking the given node with its neighbors. That is, each particle moves exactly to one of the neighbor nodes at one time step. (In following, the distance between neighbor nodes and the time step Δt are assumed unity.) There are at most one particle with given velocity vector at the node (exclusion principle). Let us denote the number of particles moving in the direction of $\mathbf{e}_k$ by n_k. Its possible values are $n_k = \{0, 1\}$, therefore, the presence at a node of particle with given velocity vector can be coded by one bit, and the state of whole node

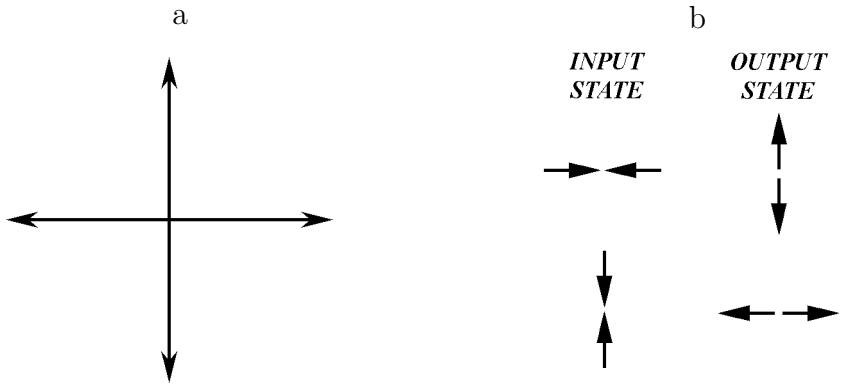

Figure 1.1. Possible velocity vectors in the HPP model (a) and possible collisions with different initial and final states (b)

— by b-digit binary number [1].

Time evolution of the system proceeds as follows. The complete time step consists of the propagation and collision sub-steps. At the propagation sub-step, each particle moves to the nearest node in the direction of its velocity. At the collision sub-step, all particles at a node interact and change their velocity directions thus that the number of particles (density $\rho = \sum_{k=1}^{b} n_k$) and the total momentum $\rho\mathbf{u} = \sum_{k=1}^{b} n_k\mathbf{c}_k$ are conserved. Each of the sub-steps can be realized using the pre-computed look-up tables. The evolution equation for the LGA method is given by

$$n_k(\mathbf{x} + \mathbf{e}_k, t + 1) - n_k(\mathbf{x}, t) = \Omega_k(n(\mathbf{x}, t)),$$

where $\Omega_k(n(\mathbf{x}, t))$ is the collision operator, i.e., the change in n_k as a result of collisions at a node. Thus, the lattice gas method is an extremely simplified version of the molecular dynamics method for the special particles with simple properties.

Historically, the first lattice gas model was the HPP model, named by its authors — Hardy, de Passiz, Pomeau [15]. Here, the square lattice is used, 4 possible velocity vectors exist (fig. 1.1,a). The only non-trivial collisions in the HPP model satisfying the conservation laws are easily seen to be "head-to-head" collisions resulting in the rotation of particle velocities by 90° (fig. 1.1,b). Unfortunately, the HPP model although behaves like a liquid, has some inadequate features. The cause of its shortcomings is the insufficient symmetry of

[1]The increase in the number of particles with given velocity vector is inexpedient because it leads to a significant complication of the computational scheme giving no substantial improvement. In the limit of $n_k = \{0, \ldots, \infty\}$, one obtains the same equations as in the lattice Boltzmann method which is substantially simpler and more obvious.

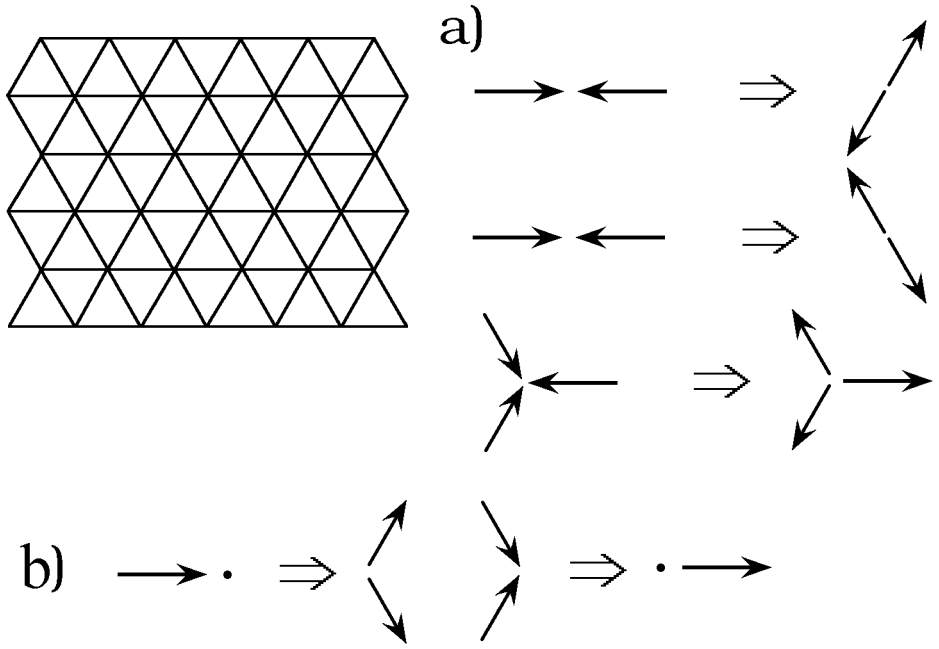

Figure 1.2. Lattice geometry and examples of possible collisions in the FHP-I model (a), some possible collisions with rest particles in the FHP-III model (b)

the square lattice. In particular, the momentum flux tensor is given by [19]

$$\Pi_{ik} = p\delta_{ik} + \rho g(\rho) \begin{pmatrix} u_x^2 - u_y^2 & 0 \\ 0 & u_y^2 - u_x^2 \end{pmatrix}.$$

Here $p(\rho)$ is the pressure, $g(\rho)$ is some coefficient. One can see, that the dynamic part of this tensor differs significantly from the usual form $\rho u_i u_k$.

Triangular lattice has, however, sufficient symmetry. The triangular lattice with $b = 6$ velocity vectors was used in [16] (FHP model — Frish, Hasslacher, Pomeau). In this case, the nontrivial collisions are the collisions of three particles with zero total momentum (the velocities are reversed after the collision), and the two- and four-particle collisions also with zero total momentum (in this case, the state is rotated by $\pi/3$ clockwise or counterclockwise, the direction is chosen randomly). This model is called FHP-I, the lattice geometry and some possible particle collisions are shown in fig. 1.2,a. The equation of state $p = \rho/2$ (up to the first order of u) corresponds to the ideal gas with constant temperature $T = 1/2$. Rest particles (at most one per site) can exist in the extended model FHP-III, also proposed in [16]. Rest particles can turn into moving ones in collisions, and vise versa (fig. 1.2,b). In this case, the pressure is $p = 3/7\rho$.

It was shown in [16], that this simple system simulates the equations of the

Navier–Stokes type (averaged over a macroscopic space-time region)

$$\frac{\partial u_\alpha}{\partial t} + g(\rho)u_\beta \frac{\partial u_\alpha}{\partial x_\beta} = -\frac{1}{\rho}\frac{\partial p}{\partial x_\alpha} + \nu(\rho)\Delta u_\alpha.$$

Here $g(\rho)$ is some coefficient (e.g., in the FHP-I model $g = (3-\rho)/(6-\rho)$), $\nu(\rho)$ is the kinematic viscosity, greek indices α, β denote cartesian coordinates, sum over repeated indices is assumed. The pressure is $p(\rho, u) = \rho/2 - \rho g u^2$.

In contrast with the HPP model, here the averaged equations are isotropic, the lattice structure is dropped out at the averaging. Similarly, high-symmetry crystals behave as isotropic solids.

Shortcomings of the model — the lack of Galilean invariance(coefficient $g(\rho) \neq 1$ before the convective term) and the unphysical velocity dependence of pressure origin from the form of the collision term. These drawbacks are insignificant for low-velocity flows. In almost incompressible case, one can get rid of the coefficient $g(\rho)$ by the velocity rescaling [16].

The use of the square lattice is possible that is more convenient as the triangular one but this requires to increase the number of states. The square lattice was used in [20] with the possible velocity values of 0 (the number at a node n_0, the energy 0), 1 (n_1, the energy 1/2), and $\sqrt{2}$ (n_2, the energy 1). There are 9 possible velocity vectors, and particles have unit mass. In this model, it is possible to introduce besides the density $\rho = n_0 + n_1 + n_2$ and momentum, the full energy at a node $E = n_1/2 + n_2$, the pressure $p = E - \rho u^2/2$, and the temperature $T = p/\rho$. In this case, the energy conservation should also hold in collisions. Some examples of collisions are shown in fig. 1.3.

A great advantage of the lattice gas method is the use of integer arithmetics only. Besides the computation acceleration and economy of memory, it leads to absence of round-off errors and absolute numerical stability. It is easy in the lattice gas method to set boundary conditions of any type. For instance, at fixed boundaries one can rotate velocity of arrived particles by 180°. In this way, no-slip boundary conditions are simulated.

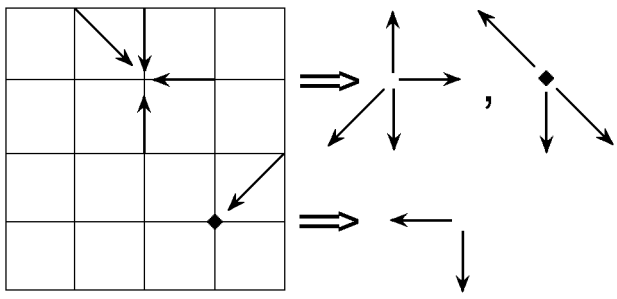

Figure 1.3. Lattice geometry and collision examples for the square lattice

The main drawback of the LGA method is the substantial statistic noise. It makes necessary to average computation results over large spatial regions, or for long time intervals, or over many copies of the system (ensemble averaging).

Moreover, there is no regular lattice with necessary symmetry in a three-

dimensional space. Therefore, it was suggested to simulate three-dimensional flows with use of the four-dimensional lattice (face-centered hypercubic) with one layer and periodic boundary conditions in the fourth dimension [21]. Then, the velocities are projected to the three-dimensional space. In this model (denoted 4D FCHC), there are 24 velocity vectors that greatly complicates the collision table (even when each collision has the single result, the size of the table is $3 \cdot 2^{24} = 48$ MB). Another variant also introduced in [21] uses the three-dimensional cubic lattice and three values of velocity 0, 1, and $\sqrt{2}$, 19 velocity vectors at the whole. In this case, the total energy should also be conserved at collisions.

To simulate multiphase and multicomponent flows, the models with inter-particle interactions were developed. The interaction can be both a repulsion between particles of different types at one node that leads to the separation of immiscible liquids [22], and a long-range attraction between particles at different nodes that allows one to simulate phase transitions [23]. The review of this class of models is given in [24].

1.2 Lattice Boltzmann equation method

The lattice Boltzmann equation method was at first developed from the LGA method [17, 18]. Later, it was directly derived from the continuum Boltzmann equation [25–29], that strengthened the theoretical basis of the LBE method significantly.

The basic idea of the LBE method is the ensemble averaging in order to get rid in principle of the statistic noise. This enables to reduce significantly the number of nodes in the computation region. The one-particle distribution functions N_k (real variables) which are the ensemble-averaged values of occupancies are used instead of binary occupancy values. Their evolution proceeds formally in the same way as in the LGA model, i.e., equations are given by

$$N_k(\mathbf{x} + \mathbf{e}_k, t + \Delta t) - N_k(\mathbf{x}, t) = \Omega_k(N(\mathbf{x}, t)), \tag{1.1}$$

where Ω_k is the collision operator. In fact, the Boltzmann kinetic equation for a certain simple model system is solved. Like LGA, the LBE method results in the Navier–Stokes equations after averaging over a space-time region.

In early works, the same collision operator as in the LGA method was used [17] (the collision operator corresponds to the collision integral in the linetic equation). Such scheme inherits all shortcomings of the LGA method — the lack of Galilean invariance and the unphysical velocity dependence of pressure.

Moreover, the collision operator consists in this case of a sum of polynoms in the form of $\prod_{k=1}^{b} N_k^{\alpha_k}(1-N_k)^{1-\alpha_k}$, $\alpha_k = \{0,1\}$, this leads both to the large number of arithmetic operations, and to the significant roundoff errors. The linearized form of the collision operator was introduced in [18] obtained by the expansion of distribution functions around their equilibrium values N_k^{eq} for the case of small Mach and Knudsen numbers. The linearized collision operator is given by $\Omega_k = \sum_{j=1}^{b} M_{kj}(N_k - N_j^{eq})$, where $\|M_{kj}\|$ is a matrix $b \times b$. It was shown in this work that taking into account the lattice symmetry and the mass and momentum conservation laws, the matrix $\|M_{kj}\|$ contains only two independent elements for the FHP-I model, and three — for the FHP-III and 4D FCHC models.

Presently, the BGK-form of the collision operator is mainly used, that was introduced for the problems of physical kinetics in 1954 (Bhatnagar, Gross, Krook [30]). It is the relaxation to the local equilibrium

$$\Omega_k(N) = -(N_k - N_k^{eq})/\tau, \tag{1.2}$$

i.e., the collision matrix is reduced to the simplest form $M_{kj} = -\frac{1}{\tau}\delta_{kj}$. The relaxation time τ governs the transport coefficients: viscosity (kinematic viscosity ν), heat conductivity and diffusivity D. Values of $\tau < 1$ imply upper relaxation. This form of the collision operator ensures Galilean invariance and can be easily extended to the three-dimensional case [31].

Equilibrium distribution functions N_k^{eq} depend on the density $\rho = \sum_{k=1}^{b} N_k$ and the mass velocity at a site $\mathbf{u} = \sum_{k=1}^{b} N_k \mathbf{c}_k/\rho$ thus that the mass, momentum and energy conservation laws are satisfied at collisions. Equilibrium distribution functions are usually chosen in the Maxwellian form: $N_k^{eq} \sim \exp(-(\mathbf{c}_k-\mathbf{u})^2/2T)$ (particle mass is assumed unity, $m = 1$). Expanding the exponential up to $O(u^2)$ one obtains

$$N_k^{eq} = \rho w_k \left(1 + \frac{\mathbf{c}_k\mathbf{u}}{T} + \frac{(\mathbf{c}_k\mathbf{u})^2}{2T^2} - \frac{u^2}{2T}\right).$$

Weight coefficients $w_k \sim \exp(-\mathbf{c}_k^2/2T)$ depend only on the value of $|\mathbf{c}_k|$.

Following equations should hold:

$$\sum_{k=1}^{b} N_k^{eq} = \rho, \qquad \sum_{k=1}^{b} N_k^{eq}\mathbf{c}_k = \rho\mathbf{u}, \qquad \sum_{k=1}^{b} N_k^{eq}\mathbf{c}_k^2 = \rho(Td + u^2).$$

Here d is the dimension of space. After the substitution of the expansion of N_k^{eq}, one should separately equate the coefficients at each power of u.

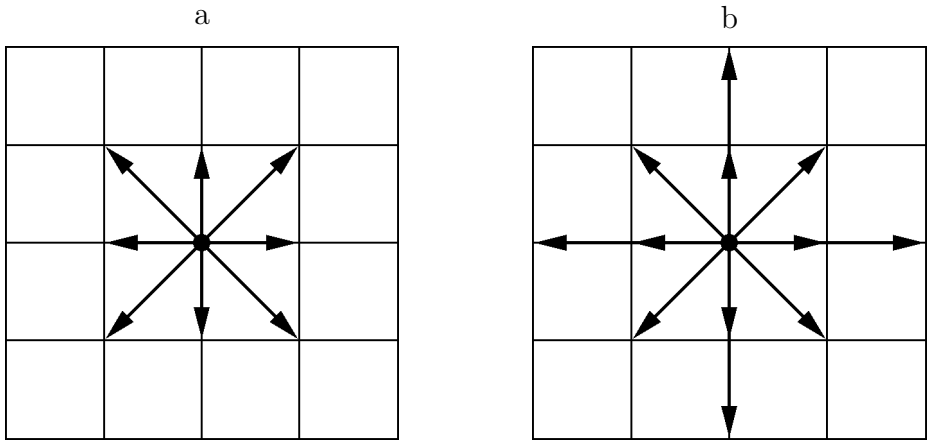

Figure 1.4. Lattice geometry and possible velocity vectors. *a* — the model with 3 velocity values (9 velocity vectors, isothermal model), *b* — the model with 3 velocity values (13 velocity vectors, variable temperature) [32]

For the one-dimensional model, $\mathbf{c}_0 = 0$, $\mathbf{c}_1 = -1$, $\mathbf{c}_2 = 1$, and one obtains $T = 1/3$, $w_0 = 2/3$, $w_{1,2} = 1/6$. In the two-dimensional model at the square lattice with 9 directions (fig. 1.4,*a*), three values of particle velocity 0, 1 and $\sqrt{2}$ are possible. This adds one more equation $w(0)/w(1) = w(1)/w(\sqrt{2})$. The solution gives $T = 1/3$, $w(0) = 4/9$, $w(1) = 1/9$, $w(\sqrt{2}) = 1/36$. Such models describe isothermal liquid flows. The sound velocity is $c_s = \sqrt{T} = 1/\sqrt{3}$. At low velocity, the liquid can be considered almost incompressible (compressibility effects are proportional to the second order of Mach number).

Using the Chapman–Enskog expansion [33] up to $O(u^2)$ of equations (1.1) and (1.2), the Navier–Stokes equations for incompressible liquid are obtained:

$$\frac{\partial \rho}{\partial t} + \frac{\partial \rho u_\alpha}{\partial x_\alpha} = 0,$$
$$\frac{\partial \rho u_\alpha}{\partial t} + \frac{\partial \rho u_\alpha u_\beta}{\partial x_\beta} = -\frac{\partial p}{\partial x_\alpha} + \nu \frac{\partial}{\partial x_\beta}\left(\frac{\partial \rho u_\alpha}{\partial x_\beta} + \frac{\partial \rho u_\beta}{\partial x_\alpha}\right),$$

here $p = \rho c_s^2 = \rho/3$ is the pressure, $\nu = (\tau - 1/2)/3$ is the kinematic viscosity [31]. In the absence of interparticle interaction, one obtains also $D = \nu = (\tau - 1/2)/3$. The stability condition is $1/2 < \tau < \infty$, that is equivalent to $D > 0$, $\nu > 0$. The equations obtained are exact, up to $O(u^2)$ [34].

The lattice Boltzmann equation was theoretically investigated in [35] in the case of finite Mach numbers, when the compressibility can not be neglected. The expression for the bulk viscosity was obtained, the formulas for the equilibrium distribution functions were introduced which allows one to adjust arbitrarily the bulk viscosity.

The LBE method was shown in [36] to be of second order of accuracy both over the space and time. The Courant number is $\lambda = \Delta t|\mathbf{c_k}|/|\mathbf{e_k}| = \mathbf{1}$, i.e.,

the method is marginally stable that leads to numerical instabilities at low viscosities. A simple way to overcome this instability was suggested in [37, 38]. It consists of the use of the reduced effective time step with further interpolation of distribution functions to the lattice sites. Along with the improved stability, this scheme leads to reducing the effective viscosity that allows one to increase the efficiency of simulations of flows with high Reynolds numbers.

The BGK-LBE method is widely used to simulate viscous flows [39, 40], see also the review [36]. The flow around the cylinder was simulated in [40] with Reynolds numbers up to 10^4. In this work, the additional interpolation step was introduced allowing one to use spatially nonuniform grid corresponding to the cylindrical geometry. In the works above, the results of computations by the LBE method were compared with the results obtained by other methods (in [39]), and also with the experiments (in [40]). The results agree well in all cases. An extensive comparison of the LBE method with spectral and finite-difference ones can be found in [41].

Another example of the use of the non-uniform spatial grid and the additional interpolation step can be found in [42]. The non-uniform grid and the combination of the LBE method with the finite-volume method was used in [43, 44] (finite-volume LBE, FVLBE). The method of local grid refinement with the use of a decreased time step in regions with the fine grid was suggested in [45]. In the next work of the same authors [46], it was shown that such grid refinement can lead to a significant acceleration of computations. The use of the multigrid model can also improve the efficiency of computations [47].

Different modification of the Lattice Boltzmann equation method exist which allows one to simulate, for example, problems of the magnetic hydrodynamics [48, 49], dynamics of a viscoelastic medium [50] and flows in a porous medium [51]. The most important of them are, however, the models describing the flows with variable temperature and the dynamics of multiphase and multicomponent fluids.

1.3 Simulation of thermohydrodynamic flows

Using the larger number of the velocity values in the LBE method makes it possible to introduce the local fluid temperature. In this case, equilibrium distribution functions depend on the temperature and the simulation of thermohydrodynamic flows becomes possible [52] — in this work the triangular lattice with three possible velocity values 0, 1, and 2 was used. The square lattice was used in [32, 53]. An example of lattice geometry and possible velocity vectors

for the two-dimensional case is shown in fig. 1.4,*b*. Other possible sets of particle velocities were introduced in [54]. The thermal diffusivity χ is uniquely coupled in such models with the relaxation time τ, i.e., the Prandtl number $\mathrm{Pr} = \nu/\chi$ is fixed. A generalized collision operator was introduced in [55] that allows one to simulate fluids with arbitrary Prandtl number.

This method is, however, stable only in the narrow range of temperature and velocity [56]. One of possible optimization ways is the modification of velocity set and its "decoupling" from the spatial lattice [56, 57].

Another way is the change of the equilibrium distribution functions. Instead of the expansion of Maxwellian distributions up to fourth order in velocity necessary to describe properly viscous terms in thermal flows [53], it was suggested to specify a dependence between distribution functions for different velocity values. In the special case of one-dimensional model with velocities $c_0 = 0, c_{1\pm} = \pm 1, c_{2\pm} = \pm 2$ this dependence was specified as $N_{2\pm} = \lambda_\pm N_{1\pm}$, where coefficients $\lambda_\pm = -\frac{(c_{2\pm}-u)^2-(c_{1\pm}-u)^2}{2T}$ correspond to the Maxwellian distribution [58]. This scheme allows one to extend the stability region of the method.

The variant of the LBE method proposed in [38] also allows one to increase the stability of thermohydrodynamic computations.

At present, other methods were developed for simulation of the thermal flows. One of them is based on the passive scalar transport of the temperature [59]. The more detailed description is given in section 1.5. This method is applicable to simulate inviscid flows. Its main shortcoming is that viscous heat dissipation and compression work are not taken into account. Another way is to introduce additional distribution functions for the internal energy [60, 61]. Evolution of these functions proceeds according to the LBE-like equation, viscous heat dissipation and compression work done by the pressure can be incorporated [60]. Density and momentum at a node are calculated using the LBE distribution functions for the substance. The internal energy dependence of the equilibrium state can be introduced allowing one to simulate substances with desired equation of state (e.g., the ideal gas or the Van der Waals one) [61].

1.3.1 Connection between the LBE method and differential equations

The LBE model corresponds to the system of partial differential equations for distribution functions (see, e.g., [57])

$$\frac{\partial N_k}{\partial t} + \mathbf{e}_k \cdot \nabla N_k = \Omega_k \qquad (k = 1, 2, \ldots, b).$$

This system is linear, and it can be solved by any hyperbolic solver [57, 62]. This method allows one, for example, to stabilize the unstable thermal models by introducing the artificial diffusion and viscosity [62].

Rather different approach was developed in [63]. Here, the overrelaxation was introduced at the propagation step. It was shown, that this results in the improved stability of the thermal model against long-wave perturbations due to additional numeric viscosity and heat conductivity. In some range of temperature, the model is also stable against short-wave perturbations.

1.4 Simulation of multiphase and multicomponent flows

The LBE method for simulation of immiscible liquids was firstly developed similarly to the LGA method [64, 65]. Additional forces near the interface were supplemented to the standard model along with the re-distribution of particles of different types on lattice directions, also near the interface in order to obtain the flux of particles of one type to the nodes with the majority of the same type of particles. In such models, the effective mutual diffusivity is negative. A model of partly miscible liquids with adjustable diffusivity was introduced in [66] based on this approach.

In another variant of the LBE method, an interaction was introduced between particles at different nodes (attraction or repulsion) [67–70]. Let us consider a system consisting of S different components (the case of one-component system, $S = 1$ is also included). We denote the component number by the index "s". In the simplest case, interaction exists between the nearest neighbors only. Interaction force is given by:

$$\Delta(\rho_s \mathbf{u}_s)/\tau_s = \mathbf{F}_s(\mathbf{x}) = -\sum_{s'=1}^{S} G_{ss'} \psi(\rho_s(\mathbf{x})) \sum_k \mathbf{e}_k \psi(\rho_{s'}(\mathbf{x} + \mathbf{e}_k)).$$

Here $\rho_s = \sum_k N_{sk}$, $\rho_s \mathbf{u}_s = \sum_k N_{sk} \mathbf{e}_k$ are density and momentum of component number s at the node $\mathbf{x}$. Interaction strength between different components is specified by the matrix $\|G_{ss'}\|$. If the element $G_{ss'} < 0$, there is an attraction between components s and s', otherwise — a repulsion. "Effective mass" $\psi(\rho)$ should be an increasing function of ρ. In computations, we assumed $\psi(\rho) = \rho_0(1 - \exp(-\rho/\rho_0))$ (ρ_0 is some constant) [67].

Action of the force leads to the change of velocity at a node:

$$\Delta \mathbf{u}_s = \mathbf{F}_s \tau_s / \rho_s.$$

The equilibrium distribution functions for the collision operator are calculated using the changed velocity $\mathbf{u}_s = \mathbf{u}' + \Delta \mathbf{u}_s$. For the mass and momentum

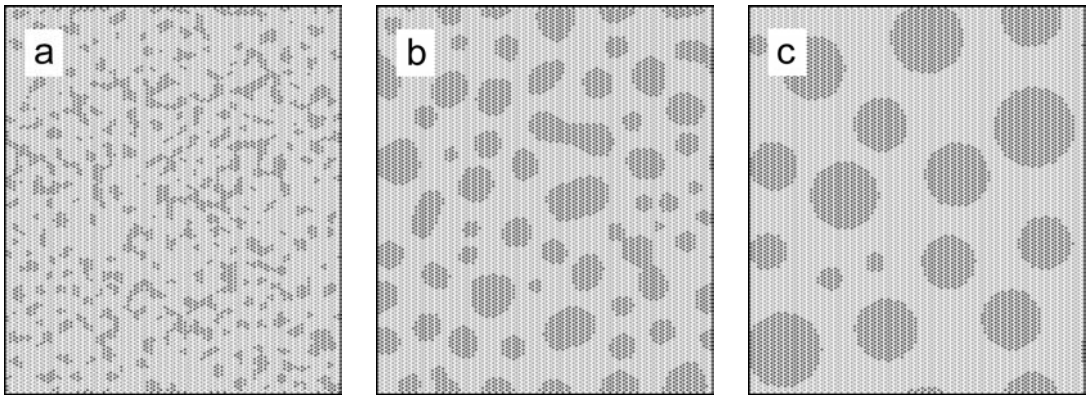

Figure 1.5. Spinodal decomposition of two immiscible liquids. $t = 6$ (a), $t = 200$ (b), and $t = 14200$ (c). Lattice size is 80×80 sites, horizontal and vertical boundary conditions are periodic

conservation laws to hold at collisions, the "common velocity" $\mathbf{u}'$ should be expressed as [69]

$$\mathbf{u}' = \frac{\sum\limits_s \rho_s \mathbf{u}_s/\tau_s}{\sum\limits_s \rho_s/\tau_s}.$$

The diffusion coefficient for multicomponent model were obtained in [69,70] in dependence on the interaction matrix $\|G_{ss'}\|$.

In this work, because of use of the square lattice (in contrast with the triangular one used in [67–70]), the interaction was also introduced between particles separated by $\sqrt{2}$, at that

$$G_{\Delta x=\sqrt{2}} = \frac{1}{8} G_{\Delta x=1}. \tag{1.3}$$

This corresponds to the force decreasing with distance as $F \sim r^{-6}$.

As a test, the spinodal decomposition was simulated — segregation of a mixture of two immiscible liquids (fig. 1.5). Here, the repulsion between different components was introduced ($G_{11} = G_{22} = 0$, $G_{12} = G_{21} > 0$).

In a certain density range, the denser substance ("liquid") can be in the equilibrium with its "saturated vapor". For this to be possible, a sufficiently strong attraction between particles should exist. Let us consider the one-component fluid and denote $G_{11} = G$. The pressure is given by formula [67]

$$p = \rho RT + \frac{b}{2} G \psi^2(\rho).$$

The critical point is determined from the equations [67]:

$$\frac{\partial p}{\partial \rho} = RT + bG_c \psi \psi' = 0,$$

$$\frac{\partial^2 p}{\partial \rho^2} = bG_c(\psi \psi' + \psi'^2) = 0,$$

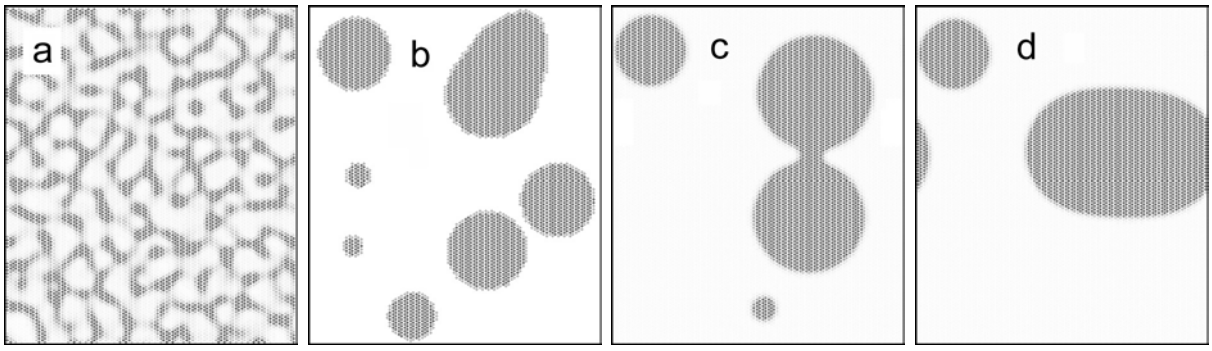

Figure 1.6. Transition from the metastable uniform state to the two-phase system "gas–liquid". $t = 26$ (a), $t = 1340$ (b), $t = 5190$ (c), and $t = 5900$ (d). Lattice size is 80×80 sites, boundary conditions at X and Y are periodic

which are analogous to the equations for the inflection point at the critical isotherm. Obviously, the simplest dependence $\psi(\rho) = \rho$ does not allow one to describe a phase transition. For the effective mass $\psi(\rho) = \rho_0(1 - \exp(-\rho/\rho_0))$, simple calculations give the critical values of $\rho_c = \rho_0 \ln 2$, $G_c = -4RT/b\rho_0$ [67]. The increase in absolute value of G is analogous to the decrease in temperature in the case of real matter.

In our case, because of use of the square lattice and two different interaction coefficients (equation (1.3)), the pressure is given by:

$$p = \frac{\rho}{3} + \frac{5}{4} G\psi^2(\rho).$$

From this equation, the critical values are $\rho_c = \rho_0 \ln 2$, $G_c = -8/15\rho_0$. Test computations were carried out which gave the value $G_c \approx -0.535$ for $\rho_0 = 1.0$ that correspond with the theoretical prediction within 0,5%.

Figure 1.6 shows the transition from the metastable uniform state to the system "liquid–gas". The formation and growth of drops is observed due to both the coalescence (fig. 1.6,c), and the evaporation of smaller drops and the vapor condensation on larger ones (fig. 1.6,b–d). At the coalescence of large drops, the form oscillations due to the surface tension are readily observed (fig. 1.6,c,d).

By a slight modification of the collision operator, a simulation of liquid-phase chemical reactions becomes possible [71]. At that, some interesting phenomena arising in reaction-diffusion systems are observable: oscillatory regimes, self-organization (generation of stable spatially non-uniform structures), autowaves, etc.

The lattice Boltzmann equation for nonideal gases was theoretically derived in [27–29] from the Enskog equation (modified Boltzmann equation for dense gases). It was shown that the expression obtained coincide with the equations of

the model introduced in [67–69] up to the terms of second order in the velocity and the interaction force. The modification of the method introduced in [27] was used in [72] to simulate three-dimensional Rayleigh–Taylor instability of two immiscible liquids.

1.5 Transport of passive scalar

A natural way exists to incorporate to the LBE method a transport of a passive scalar (admixture that does not affect the main flow). For that, an additional component with zero mass is introduced presented in the same from as the main substance. The evolution equations for the distribution function of a scalar f_k are similar to the equations for N_k:

$$f_k(\mathbf{x}+\mathbf{e}_k, t+1) - f_k(\mathbf{x}, t) = -\frac{1}{\tau_n}(f_k(\mathbf{x}, t) - f_k^{eq}(\mathbf{x}, t)).$$

The equilibrium values f_k^{eq} depend on the scalar concentration at a node $n = \sum\limits_k f_k$, and on the velocity $\mathbf{u}$ of the substance at a node (as before, $\mathbf{u} = \left(\sum\limits_k N_k \mathbf{e}_k\right) / \left(\sum\limits_k N_k\right)$, i.e., the component corresponding to the scalar introduces the zero contribution to the momentum). Thus, the transport equation for a passive scalar is obtained

$$\partial n/\partial t + \operatorname{div}(n\mathbf{u}) = \operatorname{div}(D_n \nabla n).$$

The diffusivity of passive scalar is $D_n = (\tau_n - 1/2)/3$, it can be chosen independent on the fluid viscosity. In low-velocity flows, fluid can be considered incompressible, $\operatorname{div} \mathbf{u} = 0$, and the transport equation is given by

$$\partial n/\partial t = \mathbf{u} \cdot \nabla n + \operatorname{div}(D_n \nabla n).$$

A certain disadvantage of this method is an increased amount of memory necessary for computations. This method was used, e.g., to calculate temperature in simulation of Rayleigh–Benard convection in [59].

1.6 Use of the LBE method to solve parabolic and elliptic PDEs

The variant of the LBE method described in previous section can be of independent applicability. If the flow velocity is set to zero in the whole region, the equation of parabolic type is obtained:

$$\partial n/\partial t = \operatorname{div}(\chi \nabla n).$$

Therefore, the use of this method to solve, e.g., the heat conduction equation is possible, one should only specify proper boundary conditions (in this case, n corresponds to the temperature). The thermal diffusivity $\chi = (\tau_n - 1/2)/3$ can vary over the space and time. The stability condition is $\chi > 0$. It it interesting to compare this result with the stability condition for explicit scheme $0 < \chi \Delta t/\Delta x^2 < 1/2^d$, where χ is bounded also from the other side. However, at large values of χ, the LBE method is though stable, but it gives a solution significantly different from the exact one.

If the boundary conditions are time-independent, the stationary distribution is obtained asymptotically which satisfies the Laplace equation $\mathrm{div}(\chi \nabla n) = 0$. This technique is similar to the relaxation method, it can be used to solve elliptic equations.

Thus, the LBE method is flexible and sufficiently universal computation tool to simulate different processes in fluids.

In following chapters, the LGA and LBE methods are applied to solve different hydrodynamic and electrohydrodynamic problems.